ICIC Express Letters
Volume **17**, Number **9**, September **2023**
 ISSN 1881-803X
pp. **1039–1049**

REAL-TIME LOCALIZATION OF MOBILE ROBOT USING OBSERVERS FROM LIDAR MEASUREMENT

Masahiko Shirasaya, Shohei Ueno, Yutaka Osawa and Takami Matsuo*

Department of Mechatronics
Oita University
700 Dannoharu, Oita 870-1192, Japan
{ v21e6010; ueno-shohei; v21e6005 }@oita-u.ac.jp; *Corresponding author: matsuo@oita-u.ac.jp

Received December 2022; accepted February 2023

Abstract. *In this paper, we propose a linear velocity estimator using the driftless adaptive observer with wheel encoder readings and a localization method using a nonlinear observer with landmark position signals obtained by LiDAR measurements. The proposed method is verified by MATLAB simulations and experiments with the RoboCar 1/10 manufactured by ZMP Inc., Japan.*
Keywords: SLAM, Observer, Velocity estimation, Odometry, LiDAR

1. **Introduction.** SLAM (Simultaneous Localization and Mapping) is a method combining the odometry's estimation and observations of the environment to keep the position error bounded, such as visual SLAM and LiDAR SLAM. Odometry is a simple and easy method to estimate the position and orientation of mobile robot. Odometry calibration consists of the identification of a set of kinematic parameters of wheeled mobile robots by using encoders measurements at the wheels and allows us to reconstruct the position and orientation of a vehicle body [1, 2]. The odometry is affected by three main sources of error: systematic errors such as of the modeling error, nonsystematic errors caused by wheel slippage or uneven ground, numerical drift related to discrete-time integration [2]. A systematic method for odometry calibration of differential-drive mobile robots using the kinematic equations and the least-squares method was proposed [2]. LiDAR odometry algorithms are extensively studied for vehicular positioning [3]. Gaussian filter-based and particle filters-based approaches are used in SLAM. The Kalman filter and the extended Kalman filter are widely used for multi-sensor data fusion in SLAM [1, 4, 5, 6]. Zhang et al. [7] proposed a localization method to estimate the pose of self-driving cars using a 3D-LiDAR sensor. Two separate Kalman filters are used to fuse the low-cost global positioning systems and map-matching results [7]. The observer-based approaches for SLAM have been presented using three dimensional Lie Groups [8, 9]. Medromi et al. [10] presented the state estimation of a mobile robot using the observer for bilinear systems and ultrasonic sensors. Nonaka and Watanabe [11] proposed a nonlinear observer for caster wheel odometers which estimates the translational and the rotational velocities of the mobile robots.

In this paper, we propose a linear velocity estimator using the driftless adaptive observer [12] and a localization method using a nonlinear observer with LiDAR measurements. The proposed two observer-type estimators have simpler forms and lower computational cost than the observers and the Kalman filters. In the usual LiDAR measurements, the planar coordinates have been used. To avoid the discontinuity of arctangent calculation, we use

DOI: 10.24507/icicel.17.09.1039

the Cartesian coordinates. Moreover, the experimental validation of the proposed LiDAR-based localization using a landmark is performed using the RoboCar 1/10 manufactured by ZMP Inc., Japan [13].

This paper is organized as follows. Section 2 introduces the kinematic model and the observation equation. Section 3 proposes two observers to estimate the linear velocity and the position of the mobile robot. Section 4 shows the simulation and the experimental results. Conclusion is given in Section 5.

2. **Kinematic Model and Observation.** Figure 1 shows a mobile vehicle mounted the LiDAR (Light Detection and Ranging) scanner (or Laser scanner) [1, 14]. The notations are defined as follows:

(x_c, y_c, ϕ_c): the center position and orientation of the vehicle,
(x_L, y_L): the position of LiDAR sensor,
B_i: the i-th landmark,
(x_i, y_i): the position coordinates of the i-th landmark,
$(r_i, \psi_{(\beta,i)})$: the measurement of the LiDAR sensor,
(z_{x_i}, z_{y_i}): the position coordinates of the i-th landmark in the sensor reference frame,
α: the steering angle,
ν_c: the linear speed,
L: the distance between the wheel axes.

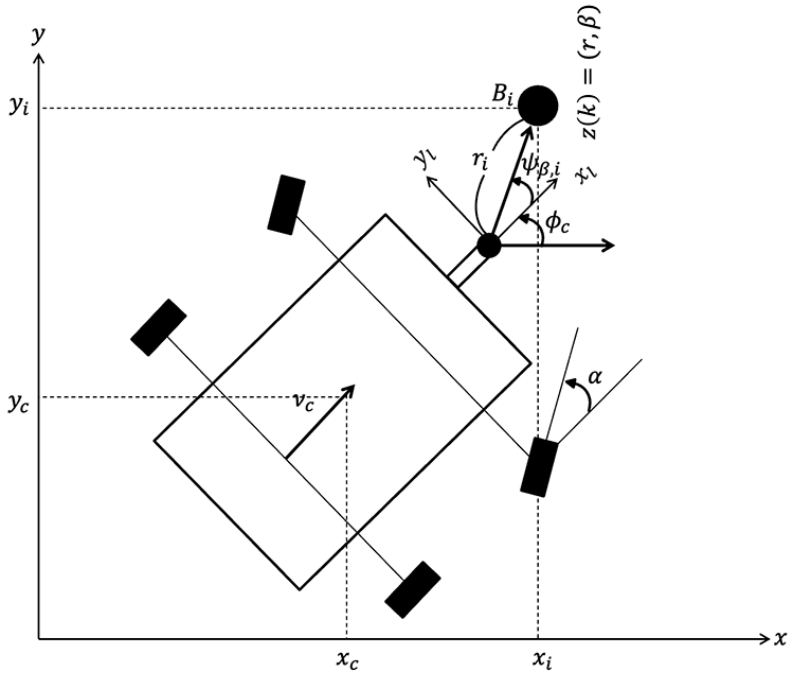

FIGURE 1. Mobile robot coordinates

The angle of the i-th landmark is given by

$$\psi_i = \psi_\beta + \phi_c$$

The kinematics of vehicle in the map coordinates [1, 14] is given by

$$\begin{bmatrix} \dot{x}_c \\ \dot{y}_c \\ \dot{\phi}_c \end{bmatrix} = \begin{bmatrix} \nu_c \cos(\phi_c) \\ \nu_c \sin(\phi_c) \\ \dfrac{\nu_c}{L} \tan(\alpha) \end{bmatrix} \tag{1}$$

The LiDAR sensor extracts the planar landmarks. The measurement vector is given by

$$\begin{bmatrix} r_i \\ \psi_{\beta,i} \end{bmatrix} = \begin{bmatrix} \sqrt{(x_i - x_L)^2 + (y_i - y_L)^2} \\ \text{atan}\left(\dfrac{(y_i - y_L)}{(x_i - x_L)}\right) - \phi_c \end{bmatrix} + \gamma_{h_i} \tag{2}$$

where γ_{h_i} is a measurement noise. The position coordinates of the i-th landmark can be written by

$$\begin{bmatrix} x_i \\ y_i \end{bmatrix} = \begin{bmatrix} \cos\phi_c & -\sin\phi_c \\ \sin\phi_c & \cos\phi_c \end{bmatrix} \begin{bmatrix} z_{x_i} \\ z_{y_i} \end{bmatrix} + \begin{bmatrix} x_L \\ y_L \end{bmatrix} \tag{3}$$

The observation equation is given by

$$\begin{bmatrix} z_{x_i} \\ z_{y_i} \end{bmatrix} = \begin{bmatrix} \cos\phi_c & \sin\phi_c \\ -\sin\phi_c & \cos\phi_c \end{bmatrix} \begin{bmatrix} x_i - x_L \\ y_i - y_L \end{bmatrix} \tag{4}$$

The linear speed of the vehicle, ν_c, is expressed as

$$\nu_c = \boldsymbol{\theta}^T \boldsymbol{\omega}(t) \tag{5}$$

$$\boldsymbol{\theta} = \begin{bmatrix} \dfrac{r_R}{2} \\ \dfrac{r_L}{2} \end{bmatrix}, \quad \boldsymbol{\omega}(t) = \begin{bmatrix} \omega_R \\ \omega_L \end{bmatrix} \tag{6}$$

where r_R, r_L and ω_R, ω_L are the right and the left radii and the angular velocities of the right and the left wheels, respectively.

We assume that

- The radii, r_R, r_L are unknown,
- The signals ω_R, ω_L are available,
- The signals $\left(r_i, \psi_{(\beta,i)}\right)$ and (x_i, y_i) are available,
- The distance between the center and the sensor is zero,
- The parameters α and L are known, and
- The displacement along the trajectory (i.e., arc length), $q(t)$ is obtained by the odometer.

Our aim is as follows:

- The linear speed ν_c using the signals ω_R, ω_L and $q(t)$ is estimated via the driftless adaptive observer, and
- The position and orientation of the vehicle are estimated using the estimated linear speed and the measurement of a landmark with the LiDAR sensor via a nonlinear observer.

3. Speed Estimation and Localization by Observers.

3.1. Linear speed estimation by driftless adaptive estimator.

The relationship between the arc length $q(t)$ and the linear speed ν_c is given by

$$\dot{q}(t) = \nu_c \tag{7}$$

The state space equation of the wheel rotational kinematics can be expressed in the driftless form:

$$\dot{q}(t) = \boldsymbol{\omega}(t)^T \boldsymbol{\theta} \tag{8}$$

$$y(t) = q(t) + \nu(t) \tag{9}$$

where $y(t)$ is the measurement output and $\nu(t)$ is the measurement noise. We estimate the unknown parameter θ by using the driftless adaptive observer proposed in [12]. The observer and the parameter update law are given by

$$\dot{\hat{q}} = -k_0 \bar{e}(t) + \boldsymbol{\omega}^T(t)\hat{\boldsymbol{\theta}} + \boldsymbol{z}^T(t)\dot{\hat{\boldsymbol{\theta}}} \tag{10}$$

$$\dot{\boldsymbol{z}}(t) = -k_0 \boldsymbol{z}(t) + \boldsymbol{\omega}(t) \tag{11}$$

$$\bar{e}(t) = \hat{q}(t) - y(t) \tag{12}$$

$$\dot{\hat{\boldsymbol{\theta}}} = -\gamma(t)\boldsymbol{z}(t)\bar{e}(t) \tag{13}$$

$$\dot{\gamma} = -\gamma^2(t)\nu(t) \tag{14}$$

$$\nu(t) = -\frac{\delta_2}{\gamma(t)} + \delta_1\bar{e}^2(t) \tag{15}$$

where $\hat{q}(t)$ is the estimate of the arc length, $\boldsymbol{z}(t)$ is the state variable filter, $\gamma(t)$ is an adaptive gain, and δ_1, δ_2 are positive constants. The estimate of the linear speed is given by

$$\hat{\nu}_c(t) = \dot{\hat{q}}(t) \tag{16}$$

3.2. **Position estimation by nonlinear observer.** Using the estimate of the linear speed and defining the state variable as

$$\boldsymbol{X}(t) = \begin{bmatrix} x_c(t) \\ y_c(t) \\ \phi_c(t) \end{bmatrix} \tag{17}$$

we have the state space equation of the mobile kinematics:

$$\dot{\boldsymbol{X}} = \begin{bmatrix} \dot{x}_c \\ \dot{y}_c \\ \dot{\phi}_c \end{bmatrix} = F(\boldsymbol{X}) = \begin{bmatrix} f_1(\phi_c, \hat{\nu}) \\ f_2(\phi_c, \hat{\nu}) \\ f_3(\phi_c, \hat{\nu}, \alpha) \end{bmatrix} = \begin{bmatrix} \cos(\phi_c) \\ \sin(\phi_c) \\ \dfrac{1}{L}\tan(\alpha) \end{bmatrix} \hat{\nu}_c(t) \tag{18}$$

In the usual SLAM setting, the planar coordinates for the measurements have been used. To avoid the discontinuity of arctangent calculation, we use the Cartesian coordinates. Assuming that the LiDAR is mounted at the center of the vehicle and the measurement information is provided by single landmark, the output equation is given by

$$\boldsymbol{Z} = \begin{bmatrix} z_1 \\ z_2 \end{bmatrix} = H(\boldsymbol{X}) + \gamma_m = \begin{bmatrix} \cos\phi_c & \sin\phi_c \\ -\sin\phi_c & \cos\phi_c \end{bmatrix} \begin{bmatrix} x_i - x_c \\ y_i - y_c \end{bmatrix} + \gamma_m \tag{19}$$

where γ_m is a measurement noise. We employ the observer to estimate the position and the orientation of the vehicle as

$$\dot{\hat{\boldsymbol{X}}} = F\left(\hat{\boldsymbol{X}}\right) + K\left(Z - H\left(\hat{\boldsymbol{X}}\right)\right) \tag{20}$$

$$\hat{\boldsymbol{Z}} = H\left(\hat{\boldsymbol{X}}\right) \tag{21}$$

where K is the observer gain, $\hat{\boldsymbol{X}}$ and $\hat{\boldsymbol{Z}}$ are the estimates of the states and outputs, respectively. The observer gain is derived from the linearized state space and output equations. We assume that the operation point, $\begin{bmatrix} \hat{x}_{c0} & \hat{y}_{c0} & \hat{\phi}_{c0} \end{bmatrix}$, satisfies

$$\Delta\hat{x}_c = \hat{x}_c - \hat{x}_{c0} \tag{22}$$

$$\Delta\hat{y}_c = \hat{y}_c - \hat{y}_{c0} \tag{23}$$

$$\Delta\hat{\phi}_c = \hat{\phi}_c - \hat{\phi}_{c0} \tag{24}$$

We have the following linearized equations:

$$\begin{bmatrix} \Delta\dot{\hat{x}}_c \\ \Delta\dot{\hat{y}}_c \\ \Delta\dot{\hat{\phi}}_c \end{bmatrix} = \begin{bmatrix} 0 & 0 & -\hat{\nu}_c\sin\hat{\phi}_{c0} \\ 0 & 0 & \hat{\nu}_c\cos\hat{\phi}_{c0} \\ 0 & 0 & 0 \end{bmatrix} \begin{bmatrix} \Delta\hat{x}_c \\ \Delta\hat{y}_c \\ \Delta\hat{\phi}_c \end{bmatrix} + K\left(z - \begin{bmatrix} -1 & 0 & 0 \\ 0 & -1 & 0 \end{bmatrix} \begin{bmatrix} \Delta\hat{x}_c \\ \Delta\hat{y}_c \\ \Delta\hat{\phi}_c \end{bmatrix}\right)$$

$$K = \begin{bmatrix} k_{11} & k_{12} \\ k_{21} & k_{22} \\ k_{31} & k_{32} \end{bmatrix}$$

The stability condition is

$$\begin{bmatrix} 0 & 0 & -\hat{\nu}_c \sin\hat{\phi}_{c0} \\ 0 & 0 & \hat{\nu}_c \cos\hat{\phi}_{c0} \\ 0 & 0 & 0 \end{bmatrix} - K \begin{bmatrix} -1 & 0 & 0 \\ 0 & -1 & 0 \end{bmatrix}$$

Selecting K as

$$K = \begin{bmatrix} k_{11} & k_{12} \\ k_{21} & 0 \\ k_{31} & 0 \end{bmatrix}$$

the characteristic equation is given by

$$\lambda^3 - k_{11}\lambda^2 + \left(k_{31}\hat{\nu}_c \sin\hat{\phi}_{c0} - k_{12}k_{21}\right)\lambda - k_{12}k_{31}\hat{\nu}_c \cos\hat{\phi}_{c0} = 0$$

The observer gain K is chosen as

$$\begin{aligned} k_{11} &= -\delta_1 = -0.01^2 \\ k_{12} &= \delta_2 \mathrm{sgn}\left(\hat{\nu}_c \cos\hat{\phi}_{c0}\right) = 0.01\mathrm{sgn}\left(\hat{\nu}_c \cos\hat{\phi}_{c0}\right) \\ k_{21} &= -\delta_3 \mathrm{sgn}\left(\hat{\nu}_c \cos\hat{\phi}_{c0}\right) = -0.001\mathrm{sgn}\left(\hat{\nu}_c \cos\hat{\phi}_{c0}\right) \\ k_{31} &= -\delta_4 \mathrm{sgn}\left(\hat{\nu}_c \sin\hat{\phi}_{c0}\right) = -0.001\mathrm{sgn}\left(\hat{\nu}_c \sin\hat{\phi}_{c0}\right) \end{aligned}$$

where the signum function is used to avoid changing the sign of coefficients of the characteristic equation.

4. **Simulation and Experimental Results.** The performance verification of the proposed method is done by computer simulations and experiments.

4.1. **Simulation result.** We verify the performance of the nonlinear observer via MATLAB/Simulink. To estimate the position of the vehicle, we use single landmark such as $x_1 = 1$, $y_1 = 3$. The measurement noise of the LiDAR sensor is the white Gaussian noise of the mean zero and the variation 0.01. First, we select the following simulation parameters: $\nu_c = 0.1$, $\alpha = 0.2$, $\sin 0.1t$, $L = 0.3$, and then the linear velocity is changed to $\nu_c = 1$. Figures 2-6 are the results for $\nu_c = 0.1$. Figures 2 and 3 show the position

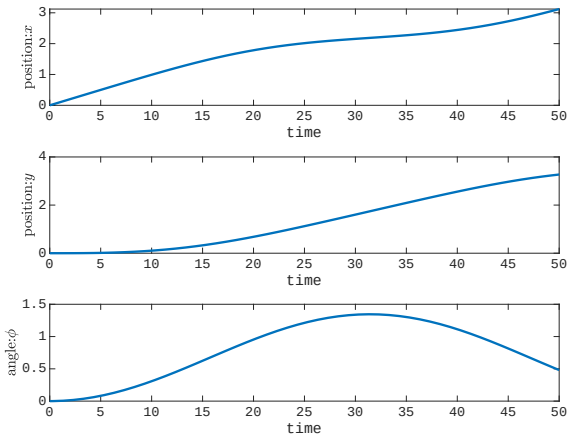

FIGURE 2. The position and the orientation for $\nu_c = 0.1$, (top) $x(t)$, (middle) $y(t)$, (bottom) $\phi(t)$

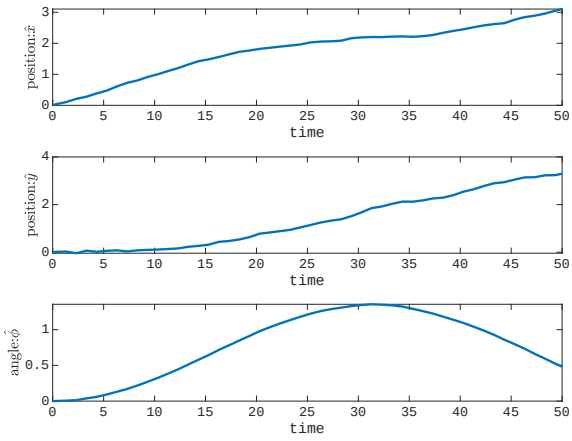

FIGURE 3. The estimates of position and the orientation for $\nu_c = 0.1$, (top) $\hat{x}(t)$, (middle) $\hat{y}(t)$, (bottom) $\hat{\phi}(t)$

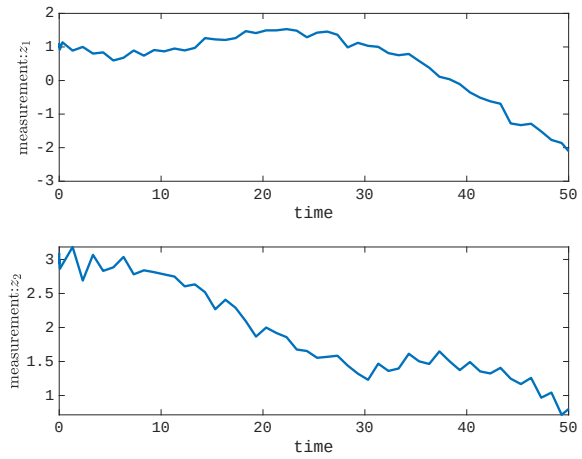

FIGURE 4. The outputs in Cartesian coordinates for $\nu_c = 0.1$, (top) $z_1(t)$, (bottom) $z_2(t)$

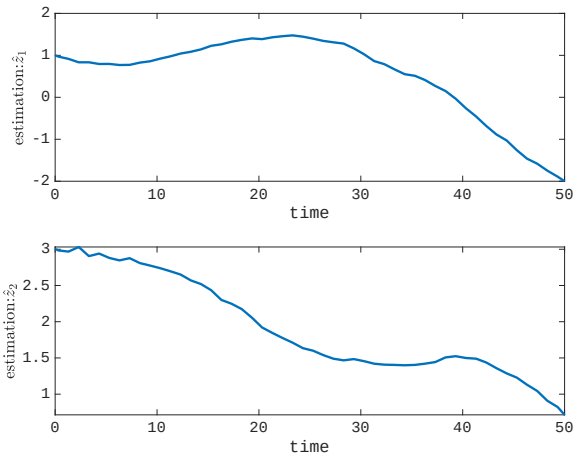

FIGURE 5. The estimates of the outputs for $\nu_c = 0.1$, (top) $\hat{z}_1(t)$, (bottom) $\hat{z}_2(t)$

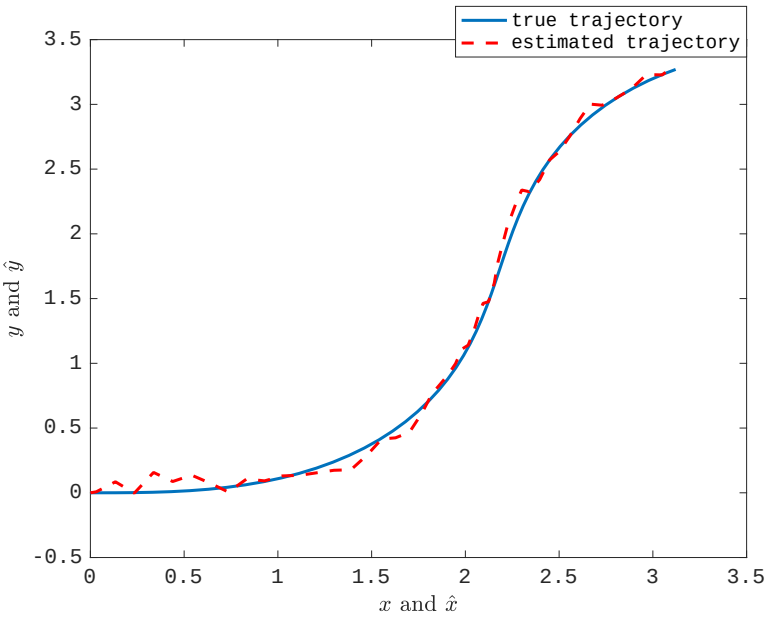

FIGURE 6. The vehicle trajectory (solid line) and its estimate (dotted line) for $\nu_c = 0.1$

and the orientation of the vehicle, and their estimates. Figures 4 and 5 show the outputs converted from Polar Coordinates to Cartesian Coordinates and their estimates. Figure 6 shows the trajectory of the vehicle and its estimate. Figures 7-11 are the results for $\nu_c = 1$. The proposed observer is less susceptible to noise in both fast and slow speed cases.

4.2. **Experimental result.** We verify the performance of the nonlinear observer by using the RoboCar from ZMP Inc. depicted in Figure 12 [13]. A monocular camera and a laser range sensor are mounted on a 1/10 scale vehicle of an automobile, and the behavior and mileage of the vehicle can be grasped by the acceleration/gyro sensor and encoder [13].

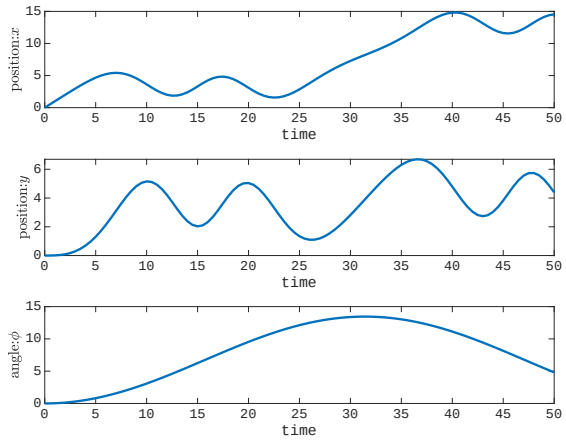

FIGURE 7. The position and the orientation for $\nu_c = 1$, (top) $x(t)$, (middle) $y(t)$, (bottom) $\phi(t)$

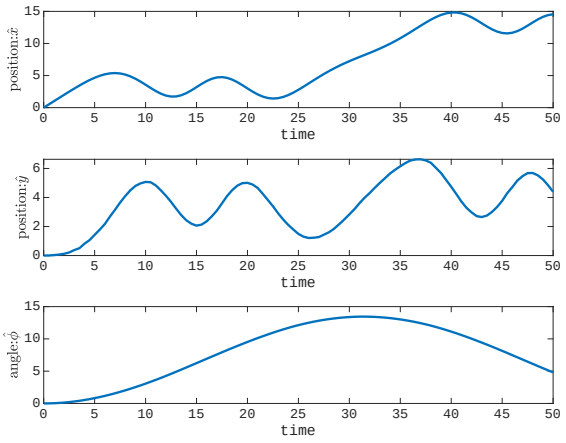

FIGURE 8. The estimates of position and the orientation for $\nu_c = 1$, (top) $\hat{x}(t)$, (middle) $\hat{y}(t)$, (bottom) $\hat{\phi}(t)$

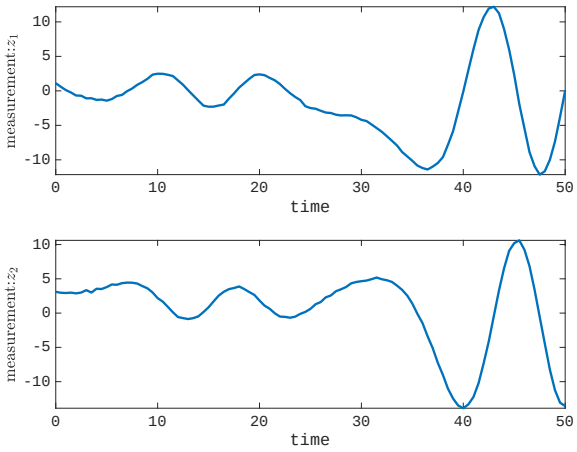

FIGURE 9. The outputs in Cartesian coordinates for $\nu_c = 1$, (top) $z_1(t)$, (bottom) $z_2(t)$

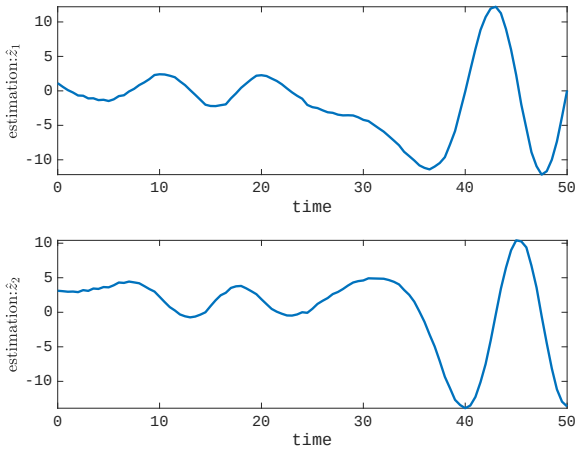

FIGURE 10. The estimates of the outputs for $\nu_c = 1$, (top) $\hat{z}_1(t)$, (bottom) $\hat{z}_2(t)$

The velocity and the steering angle are selected as $\nu_c = 50$ [mm/s], $\alpha = -10$ [deg]. Figures 13 and 14 show the position and the orientation of the RoboCar, and their estimates. The transformed outputs by the LiDAR measurements are shown in Figure 15. Their estimates by the nonlinear observer are shown in Figure 16. Figure 17 shows the trajectory and its estimate by the nonlinear observer. When the steering angel is small, the estimator works well. As the angle increased, however, the error in the estimated value becomes large.

Then, we constructed a route as shown in Figure 18 to verify the effectiveness of the method over long distances. In Figure 18, "L" mark indicates single landmark and "S" and "G" marks indicate the start point and the goal point. The landmark position is obtained by detecting the corner using the point cloud data with LiDAR measurement. Figure 19 shows the true trajectory and its estimate. Comparing Figure 18 and Figure 19, the estimation calculation is finished before the RoboCar reaches the goal. Since it becomes more difficult to measure single landmark as the RoboCar moves away from the

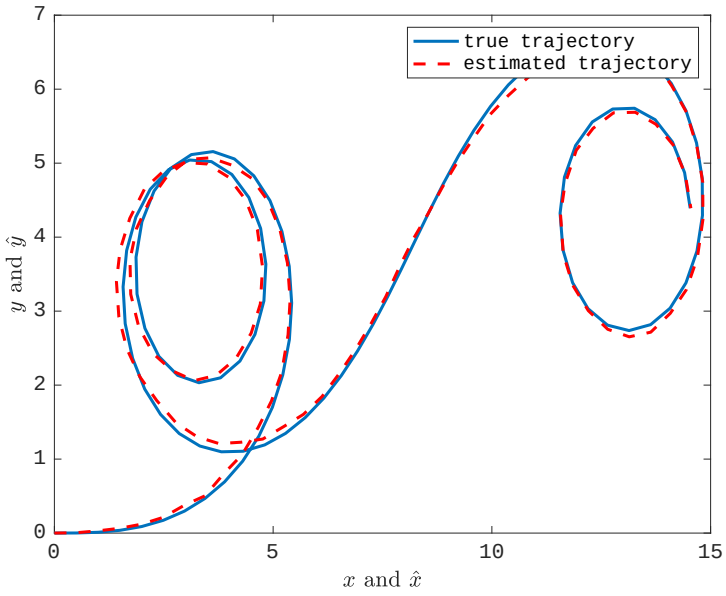

FIGURE 11. The vehicle trajectory (solid line) and its estimate (dotted line) for $\nu_c = 1$

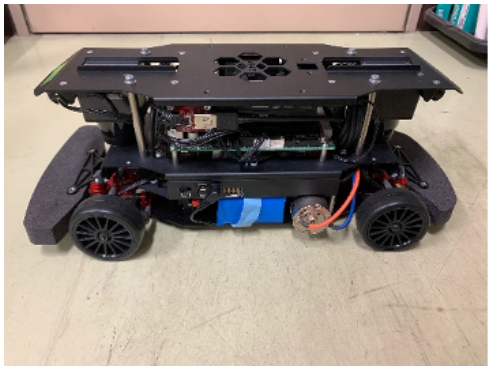

FIGURE 12. The RoboCar 1/10 from ZMP Inc. [13]

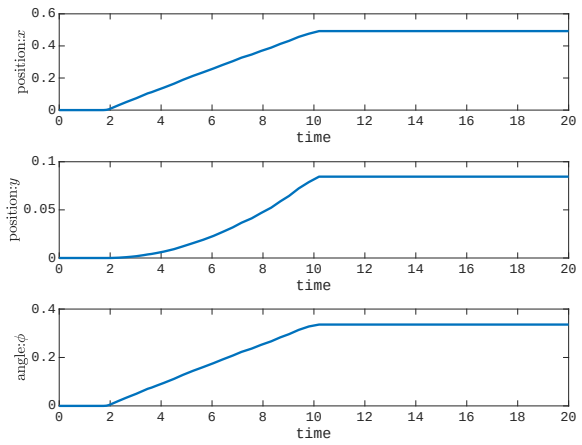

FIGURE 13. The position and the orientaion of the RoboCar, (top) $x(t)$, (middle) $y(t)$, (bottom) $\phi(t)$

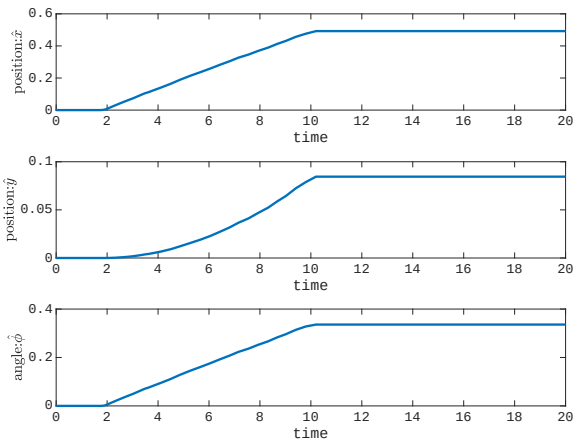

FIGURE 14. The estimates of position and the orientaion of the RoboCar, (top) $\hat{x}(t)$, (middle) $\hat{y}(t)$, (bottom) $\hat{\phi}(t)$

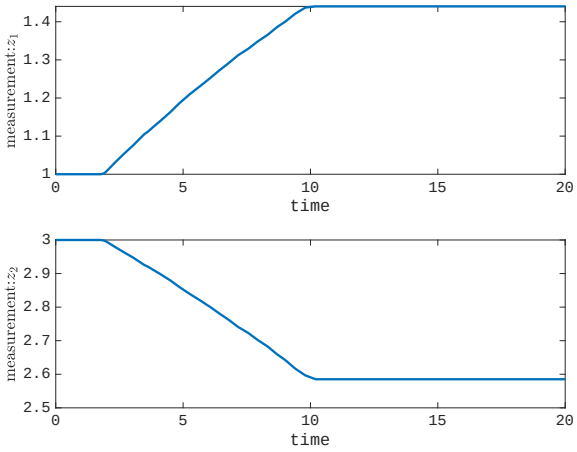

FIGURE 15. The outputs of the RoboCar in Cartesian coordinates, (top) $z_1(t)$, (bottom) $z_2(t)$

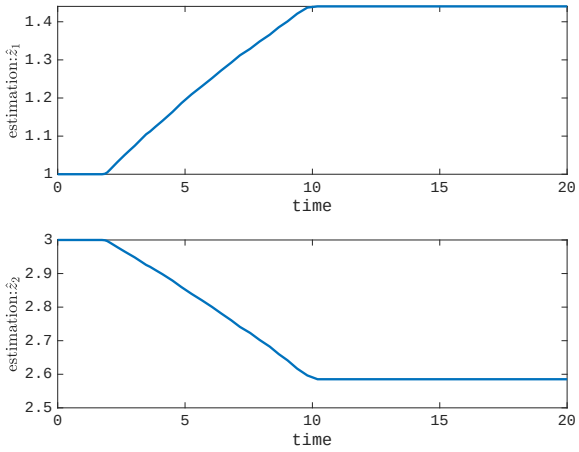

FIGURE 16. The output estimates of the RoboCar, (top) $\hat{z}_1(t)$, (bottom) $\hat{z}_2(t)$

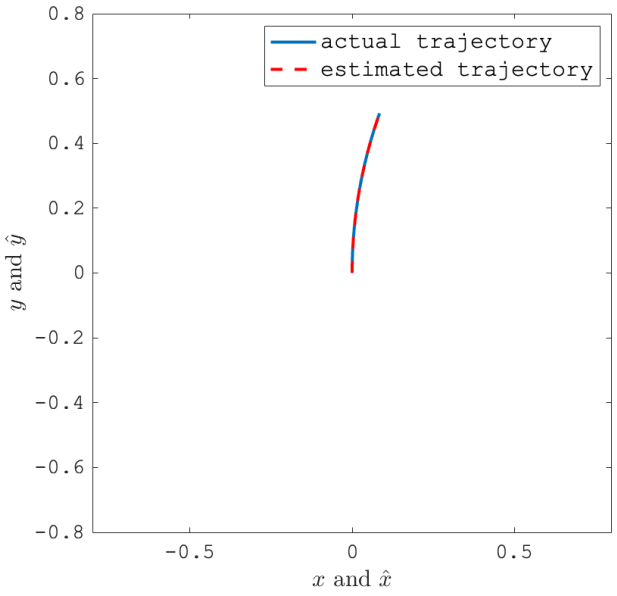

FIGURE 17. The vehicle trajectory (solid line) of the RoboCar and its estimate (dotted line)

landmark point, only up to the point where single landmark point can be measured can be estimated. It is necessary to improve the data by adding more landmarks in the future.

5. **Conclusion.** In this paper, we proposed a real-time localization algorithm consisting of a driftless adaptive observer to estimate the radii of the wheels and a nonlinear observer to estimate the position and the orientation. To avoid the discontinuity of arctangent calculation, we used the Cartesian coordinates for the LiDAR measurements. We demonstrated that the proposed estimator worked well in the case of small steering angles. The introduction of the Ackerman vehicle model is a next step of the future study.

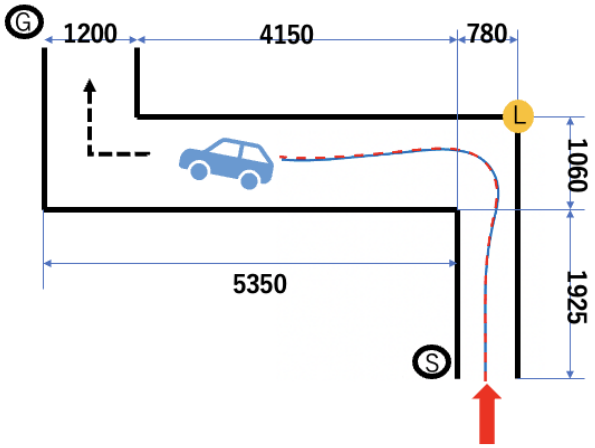

FIGURE 18. Actual driving route

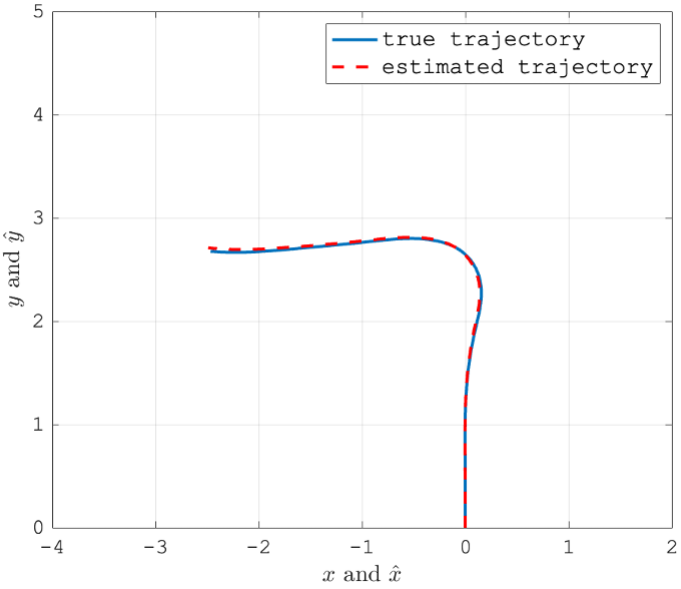

FIGURE 19. The vehicle trajectory (solid line) and its estimate (dotted line)

Acknowledgment. This work is supported by Mitsutoyo Association for Science and Technology, the Grant-in-Aid for Scientific Research ((C)22K04156), and the Grant-in-Aid for Encouragement of Scientists (22H04431).

REFERENCES

[1] J. E. Guivant and E. M. Nebot, Optimization of the simultaneous localization and map-building algorithm for real-time implementation, *IEEE Trans. Robotics and Automation*, vol.17, no.3, pp.242-257, 2001.

[2] G. Antonelli, S. Chiaverini and G. Fusco, A calibration method for odometry of mobile robots based on the least-squares technique: Theory and experimental validation, *IEEE Trans. Robotics*, vol.21, no.5, pp.994-1004, 2005.

[3] J. Zhang and S. Singh, LOAM: Lidar odometry and mapping in real-time, *Proceedings of the Robotics: Science and Systems*, vol.2, pp.1-9, 2014.

[4] Q. Zou, Q. Sun, L. Chen, B. Nie and Q. Li, A comparative analysis of LiDAR SLAM-based indoor navigation for autonomous vehicles, *IEEE Trans. Intelligent Transportation Systems*, vol.23, no.7, pp.6907-6921, 2022.

[5] F. Espinosa, C. Santos, M. M-Romera, D. Pizarro, F. Valdes and J. Dongil, Odometry and laser scanner fusion based on a discrete extended Kalman filter for robotic platooning guidance, *Sensors*, vol.11, pp.8339-8357, 2011.

[6] S. Liu, M. M. Atia, Y. Gao and A. Noureldin, Adaptive covariance estimation method for LiDAR-aided multi-sensor integrated navigation systems, *Micromachines*, vol.6, pp.196-215, 2015.

[7] Y. Zhang, L. Wang, X. Jiang, Y. Zeng and Y. Dai, An efficient LiDAR-based localization method for self-driving cars in dynamic environments, *Robotica*, vol.40, no.1, pp.38-55, 2022.

[8] J. F. Vasconcelos, R. Cunha, C. Silvestre and P. Oliveira, A nonlinear position and attitude observer on SE(3) using landmark measurements, *Systems & Control Letter*, vol.59, pp.155-166, 2010.

[9] D. E. Zlotnik and J. R. Forbes, Gradient-based observer for simultaneous localization and mapping, *IEEE Trans. Autom. Control*, vol.63, pp.4338-4344, 2018.

[10] H. Medromi, J. Y. Tigli and M. C. Thomas, Posture estimation of mobile robots: Observers-sensors, *Proc. of 1994 IEEE Int. Conf. on Multisensor Fusion and Integration for Intelligent Systems*, pp.661-666, 1994.

[11] K. Nonaka and Y. Watanabe, Velocity estimation for mobile robots using caster odometer and nonlinear observer, *Trans. of the Japan Society of Mechanical Engineers, Series C*, vol.78, no.791, pp.2509-2525, 2012.

[12] Y. Sato, T. Kodama, T. Moriyama and T. Matsuo, Noise-robust adaptive observer of driftless system and application to disturbance estimation of rotational movements in quadrotor, *Proc. of the SICE Annual Conference 2019*, pp.759-762, 2019.

[13] ZMP Inc., *Autonomous Driving Development Platform RoboCar 1/10X*, https://www.zmp.co.jp/en/products/robocar/robocar-110x, Accessed on Nov. 15, 2022.

[14] A. Chand, M. Kawanishi and T. Narikiyo, Application of sigmoidal Gompertz curves in reverse parallel parking for autonomous vehicles, *International Journal of Advanced Robotic Systems*, vol.12, no.9, pp.1-11, 2015.